minerals

MDPI

Article

Evolution of Metakaolin Thermal and Chemical Activation from Natural Kaolin

Isabel Sánchez [1], Isabel Sonsoles de Soto [2], Marina Casas [3], Raquel Vigil de la Villa [3] and Rosario García-Giménez [3,*]

1 Facultad de Ciencias, Universidad Nacional de Educación a Distancia (UNED), 28040 Madrid, Spain; isa.svigil@gmail.com
2 Departamento de Ciencias, Escuela Técnica Superior de Ingeniería Agronómica y Biociencias, Universidad Pública de Navarra, 31006 Pamplona, Spain; isabelsonsoles.desoto@unavarra.es
3 Departamento de Geología y Geoquímica, Universidad Autónoma de Madrid (UAM), 28049 Madrid, Spain; marina.casas@uam.es (M.C.); raquel.vigil@uam.es (R.V.d.l.V.)
* Correspondence: rosario.garcia@uam.es; Tel.: +34-9-1497-4819

Received: 27 April 2020; Accepted: 10 June 2020; Published: 12 June 2020

Abstract: In the present paper, we study the combined effect of thermal activation (600 °C/2 h and 750 °C/2 h) and chemical activation with 1% ZnO on the reactivity of metakaolinite (MK) obtained from natural kaolin. The phases are identified by chemical (ICP/MS), mineralogical (XRD), and morphological (SEM/EDX) characterization of all products, as well as the evolution and stability over time of the hydrated phases generated during the reaction, to determine their use as pozzolan in the manufacture of cements. The stability analysis for the kaolin/lime system activated chemically and thermally at 600 °C/2 h shows that the C-S-H gels are thermodynamically stable after one day of reaction, evolving the system to the stability field of stratlingite for the other analyzed times. At 750 °C/2 h, the thermodynamically stable reaction phases are C-S-H gels. Calcination at 600 °C/2 h and the addition of 1% ZnO are the optimal conditions for thermal and chemical activation, to improve the pozzolanic reaction and promote the replacing part of the cement for developing secondary reaction products.

Keywords: kaolinite; activated waste; stratlingite; LDH compounds; C-S-H gels; stability; geochemical code; pozzolan

1. Introduction

In the context of the circular economy, waste plays a leading role, and its revaluation becomes a priority. The use of any by-product or waste generated during an industrial process is currently of great importance from the scientific, technical, economic, energy, and environmental aspects. One of the ways available in the construction sector for the use of industrial solid waste is its incorporation as an active addition to cement. However, its use requires a great deal of research effort since, in order to be used, it must be included in the corresponding product regulations [1–4].

It is proposed to use pozzolanic additions, that is, materials with a silicon, silica–aluminum chemical composition or a combination of both that, together with dissolved calcium hydroxide, generated insoluble compounds of calcium silicate and calcium aluminate with cementing properties and chemical–physical characteristics similar to those of Portland cement [5].

The scientific community is making a great effort to recover, as much as possible, waste that can be used according to the criteria of the circular economy, proposing a significant number of industrial wastes as pozzolan alternatives. From kaolinite (K), by means of controlled thermal activation, metakaolinite (MK) can be obtained, a product with highly pozzolanic properties. Previous works on

the thermal activation (between 650 °C and 750 °C) of wastes containing K gave rise to products with high pozzolanicity [6].

Digital technologies were introduced into the design of concrete structures, and they help to complete traditional research. These innovations focus on the use of topology optimization, architectural geometry, and three-dimensional (3D) printing [7,8].

The objective of the present paper is to evaluate the combined effect of thermal and chemical activation on MK reactivity from natural K, as well as on the products of the pozzolanic reaction with transformations along time, to establish the scientific basis and the evaluation of its possible incorporation in the fabrication of cements.

This study analyzes the influence of these materials on the evolution of the pozzolanic activity and the reaction products by means of thermodynamic modeling based on speciation calculations and stability fields to predict the system stability with hydration time.

2. Materials and Methods

2.1. Materials

The main material for this study was kaolin from Burela (Lugo, Spain), which was activated thermally by calcination and chemically by adding ZnO.

The calcium hydroxide used to prepare the saturated lime solution was supplied as a powder with an extra-pure purity index (Ph. Eur., USP). ZnO, used as a chemical activator, was from PANREAC, and the TiO_2 powder, used as an internal standard, was from Aldrich, with a purity of 99.99%.

2.2. Methods

In this study, two conditions for thermal activation, 600 °C and 750 °C, were applied (initial temperature ramp of 20 °C/min and a residence time of 2 h in the oven) to transform kaolin into a pozzolanic material [9–12]. As a previous step to the kaolin calcination, mixtures were prepared via substitution of 1% of this material with 1% of ZnO as a chemical activator in the pozzolanic reaction.

The accelerated method of saturated lime dissolution was used [13–15] for the measurement of pozzolanic activity. This method is based on the standard test for pozzolanic cements (Frattini test) [16]. The chemical characterization of the solutions was performed with a Perkin Elmer brand Elan 6000 inductively coupled plasma mass spectrometer with an AS91 automatic injector.

The mineralogical composition was determined by X-ray diffraction (XRD) (SIEMENS 5000 X-ray diffractometer (Siemens, Madrid, Spain), equipped with a Cu anode. Its operating conditions were 40 mA and 45 kV, and the divergence of reception slits was 0.5° and 1/2 mm). The sample characterization was performed using the random power method operating from 5° to 70° 2θ [17] with an internal rutile standard to quantify the amorphous phase. The measured standards were analyzed using the Match v.3 and Rietveld Full Prof software with the Inorganic Crystal Structure Database (ICSD) and the Open Crystallography Database (COD).

Morphological observations and the microanalysis of samples were carried out by SEM/EDX, using the Inspect FEI Company electron microscope (FEI, Hillsboro, USA), model INSPECT, equipped with an energy dispersive X-ray analyzer (tungsten source). The powder samples were fixed to the metal sample holder by means of a graphite bi-adhesive sheet. The surface was metallized with gold to guarantee conductivity in a BIO RAD model SC 502 equipment. The chemical composition was obtained by an average value of 10 points analyzed for each sample; in this case, the value was joint with the standard deviation, using a DX4i X-ray dispersive energy (EDX) analyzer (FEI, Hillsboro, USA) and Si/Li detector. Results are expressed in oxides (% by weight), adjusted to 100%.

The thermodynamic analysis of stability in the pozzolanic reaction aims to support the hypothesis of dissolution/precipitation processes in the phases observed experimentally as reaction products. The assay begins with the calculation of the chemical speciation of the aqueous phases extracted after each system. In this way, the saturation indices (IS) of the phases in the reaction medium and, therefore,

their tendency to dissolve or precipitate are obtained. Considering these data, a reaction model is defined where reagents and products are, respectively, the most unstable phases and the most stable association under the new conditions.

Finally, once the hypothetical reaction is identified and its consistency with the experimental data is verified, the process is modeled to predict its extension, that is, to evaluate the equilibrium concentrations of the neoformation phases and those dissolved in the pozzolanic reaction.

3. Results and Discussion

3.1. Natural Kaolin

A chemical analysis was carried out on the natural kaolin sample for its characterization (Table 1).

Table 1. Chemical composition of major elements from Burela kaolin.

Oxides	SiO_2	Al_2O_3	Fe_2O_3	CaO	MgO	K_2O	Na_2O	TiO_2	P_2O_5	MnO_2	LOI
(%)	45.04	39.35	0.79	0.05	0.22	1.02	0.10	0.16	0.04	0.01	13.13

LOI = loss on ignition.

The results indicate that the main components are silica and alumina, with small amounts of potassium and iron oxides.

The proportion of CaO is low in contrast to the pozzolans of industrial waste considered in other investigations [18–23]. The Burela kaolin has a kaolinite content higher than that collected in the references and, in turn, a much lower percentage of calcite. The loss on ignition (LOI), 13.13%, is attributed to the dehydroxylation process by structural hydroxyl groups, in the 1:1 K and 2:1 micas (Table 1).

SEM/EDX indicates kaolinite and muscovite aggregates, with compact surfaces and a wide range of sizes. In the smallest aggregates, the typical laminar appearance of these phyllosilicates is clearly observed, in addition to silica-rich aggregates corresponding to quartz (Figure 1 and Table 2).

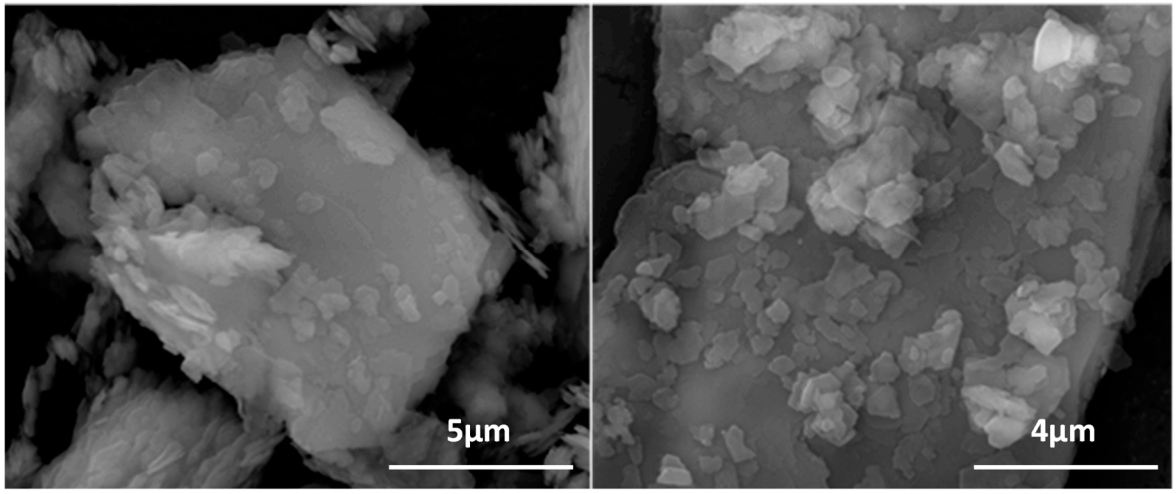

Figure 1. Kaolinite (**left**) and mica (**right**) crystals: superficial appearance.

Table 2. Chemical analysis by EDX in natural kaolin.

Oxides (%)	Muscovite	Kaolinite	Quartz
MgO	0.78 ± 0.06	n.d.	n.d.
Al_2O_3	36.11 ± 1.27	41.86 ± 1.23	n.d.
SiO_2	49.07 ± 1.38	58.14 ± 2.41	100
K_2O	11.02 ± 1.11	n.d.	n.d.
TiO_2	0.45 ± 0.,11	n.d.	n.d.
Fe_2O_3	2.57 ± 0.94	n.d.	n.d.

n.d. = not detected.

Chemical analysis by SEM/EDX (Table 2) shows Si and Al from the kaolin sample. Chemical analyses of muscovite show, in addition to silicon and aluminum, iron, potassium, titanium, and magnesium. The total SiO_2 and Al_2O_3 contents are significantly high, while the MgO, TiO_2, and Fe_2O_3 contents are very low, and the K_2O concentration is over 10%.

The mineralogical composition was identified by comparison with COD cards (Crystallography Open Database) by reading the following characteristic reflections: 10.01 Å, 5. Å, 4.48 Å, and 3.35 Å corresponding to mica ($2M_1$ muscovite); kaolinite at 7.16 Å; 4.46 Å, and 3.57 Å; quartz at 4.26 Å, 3.34 Å, and 1.81 Å (Figure 2 and Table 3).

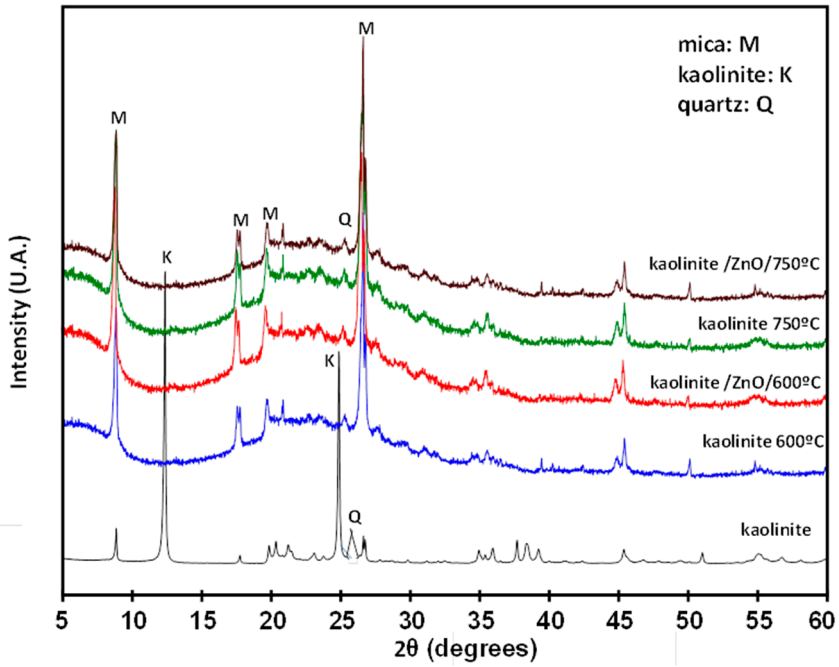

Figure 2. XRD analysis from kaolin + 1% ZnO calcined at 600 °C and 750 °C for 2 h.

Table 3. Quantification of all the phases present in natural kaolin using the Rietveld method.

	R_B	χ^2	Kaolinite (%)	Mica (%)	Quartz (%)	Amorphous Material (%)
Natural kaolin	12.3	4.9	45	30	18	7

R_B and X^2: agreement factors.

3.2. Chemical and Thermal Analysis by Activated Kaolin

Figure 2 and Table 4 show the XRD analysis of the chemically activated kaolin when adding ZnO (1%) at 600 °C and 750 °C for 2 h and their Rietveld quantification.

Table 4. Rietveld quantification of kaolin + 1% ZnO.

Samples	Temperature (°C)	R_B	X^2	Kaolinite (%)	Muscovite (%)	Quartz (%)	Amorphous Material (%)
Kaolin	600	6.3	5.8	n.d.	30	18	52
Kaolin + 1% ZnO	600	5.9	5.2	n.d.	30	18	52
Kaolin	750	7.4	6.4	n.d.	35	18	47
Kaolin + 1% ZnO	750	6.8	5.9	n.d.	35	18	47

R_B and X^2: agreement factors; n.d. = not detected.

Calcination at 600 °C/2 h shows kaolinite elimination by the total dehydroxylation process, as well as the presence MK [24,25], and it produces the initial process in the muscovite, leading to transition phases with high reactivity by partial breakdown of the crystal lattice [26,27].

In the calcination at 750 °C /2 h, the amorphous phase concentrations are minor with an increase in muscovite concentration, as well as the presence of quasi-stable partially dehydroxylated phases, while trioctahedral micas tend to dehydroxylate and recrystallize more or less at the same time [28]. The presence of quartz in natural kaolin is maintained after heat treatments.

Calcinations at 600 °C /2 h and 750 °C /2 h + 1% ZnO do not change the results observed by XRD. ZnO is not detected as a crystalline phase and does not produce variation in the quantifications.

3.3. Pozzolanic Reaction

In order to know the possibility of using MK as a pozzolanic material, pozzolanic activity was studied as described in the methodology. With this reaction, two phases are obtained, liquid and solid, which are then analyzed.

3.3.1. Solid Phase

XRD results corresponding to the study of the kinetics reaction in the pozzolan/lime systems are presented in Figure 3 and Tables 5 and 6.

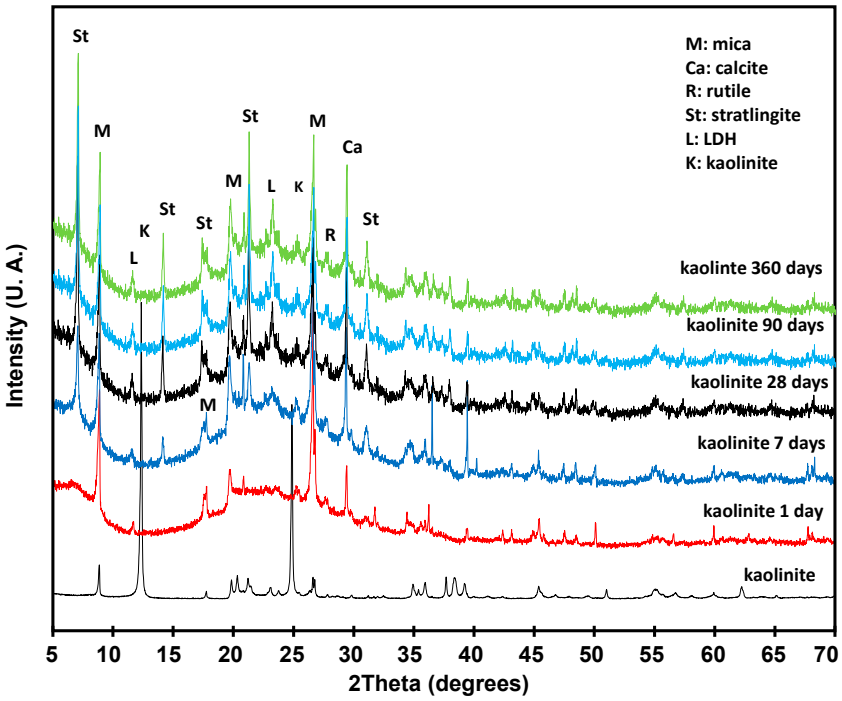

Figure 3. XRD patterns from kaolin/lime systems at one, seven, 28, 90, and 360 days of pozzolan reaction at 600 °C/2 h.

Table 5. Rietveld quantification in kaolin/lime systems at 600 °C/2 h.

Time (days)	R_B	X^2	Calcite (%)	LDH (%)	Muscovite 3T (%)	Quartz (%)	Stratlingite (%)	Amorphous Material (%)
1	8.25	6.4	12	8	39	9	n.d.	32
7	6.47	4.9	10	5	22	8	28	27
28	6.12	3.5	21	4	19	7	30	19
90	6.31	4.2	20	4	17	5	34	20
360	7.24	5.6	18	4	16	3	35	24

R_B and X^2: agreement factors; n.d. = not detected; LDH = LDH compounds (Layered double hydroxides).

Table 6. Rietveld quantification in kaolin/lime systems at 750 °C/2 h.

Time (days)	R_B	X^2	Calcite (%)	LDH (%)	Muscovite 3T (%)	Quartz (%)	Stratlingite (%)	Amorphous Material (%)
1	8.62	5.7	22	18	29	7	n.d.	24
7	7.35	6.2	18	15	25	4	31	7
28	6.47	5.9	12	13	21	n.d.	33	21
90	8.25	5.8	10	8	15	n.d.	34	33
360	5.98	6.3	9	6	11	n.d.	36	38

R_B and X^2: agreement factors; n.d. = not detected.

Using XRD, stratlingite was detected at 12.61 Å, 6.28 Å, 4.15 Å, and 2.87 Å, while LDH-type compounds (phyllosilicate/carbonate) were detected at 7.60 Å, 7.41 Å, and 3.78 Å [29]. In addition, muscovite reflections appeared at 10.01 Å, 5.03 Å, 4.48 Å, and 3.35 Å, although slightly displaced toward 9.97 Å with respect to 10.01 Å and 3.34 Å with respect to 3.35 Å. These variations suggest that the pozzolanic reaction generates the $2M_1$ muscovite restructuring toward a 3T muscovite with characteristic spacing at 9.97 Å and 3.34 Å (Figure 4).

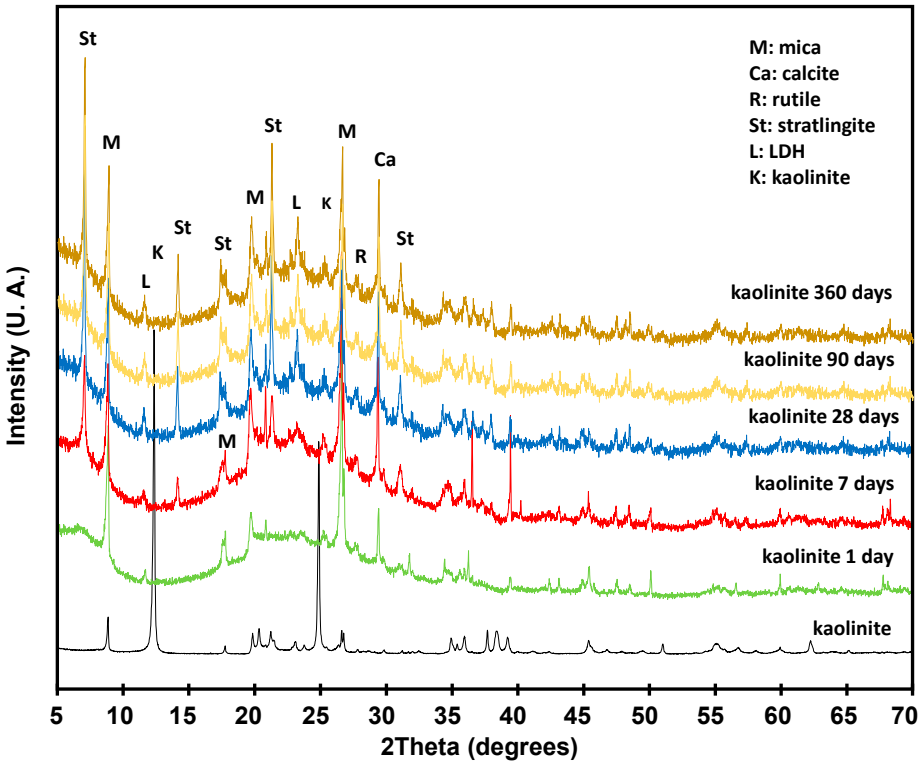

Figure 4. XRD patterns from kaolin/lime systems at one, seven, 28, 90, and 360 days of pozzolan reaction at 750 °C /2 h.

Furthermore, calcite formation was detected at 3.86 Å, 3.03 Å, 2.49 Å, 2.28 Å, 2.09 Å, 1.91 Å, and 1.87 Å, and quartz reflections were maintained at 4.26 Å, 3.34 Å, and 1.81 Å from the original material.

Calcination at 750 °C/2 h increased MK reactive and amorphous material content (Table 6). It should be noted, under these conditions, that amorphous phase content increased at long ages (28, 90, and 360 days).

The characterization of solid products from the pozzolanic reaction indicates the minimal solidification of C-S-H gels with and without aluminum in their structure [30–33]. Therefore, and since there is little literature available on the pozzolanic reaction of MK that includes specific analyses of aqueous solutions, speciation analysis and geochemical modeling of the resulting aqueous phases were then carried out, after treating the activated natural kaolin with a saturated lime solution at one, seven, 28, 90, and 360 days, to be able to predict the most stable associations.

3.3.2. Liquid Phase

Figure 5 shows the evolution of the lime content fixed in the calcined kaolin/lime systems at different reaction times.

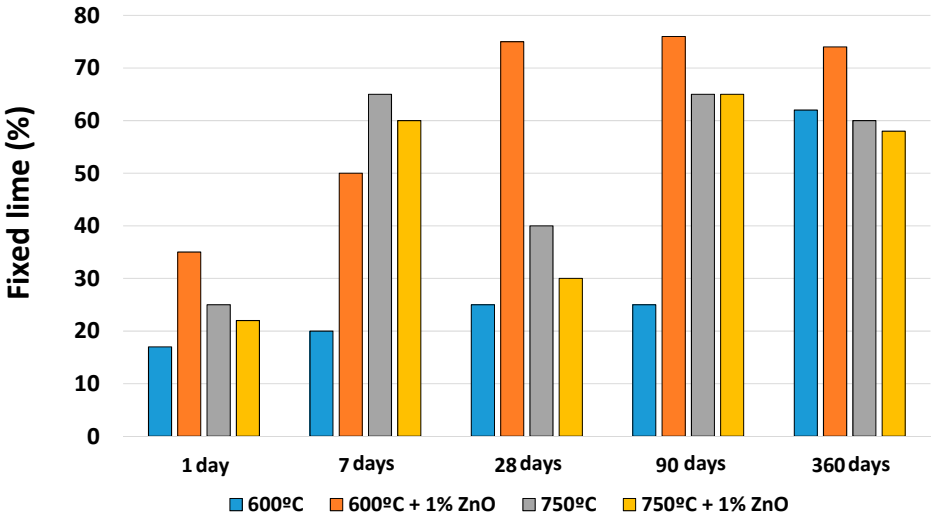

Figure 5. Fixed lime evolution with different activation conditions.

The fixed lime values for the samples calcined at both temperatures show high pozzolanic activity at all reaction times. These results correspond to a logarithmic growth up to 90 days, in which time the maximum is practically reached. This situation is comparable for all the activation conditions and for longer times.

ZnO addition before the thermal activation process produced an increase in the reactivity of MK with the calcium hydroxide of the saturated lime solution. This increase was detected at all times, mainly during the first seven days of pozzolanic reaction (Figure 5). This fact can be explained by the disaggregation in the microgranular constituents with the addition of the chemical activator [19,34,35].

The consumption of Ca^{2+} (aq.) in the solution is associated with the pozzolanic reaction, where MK reacts with the Ca^{2+} (aq.) available in the alkaline medium to form, mainly, gels without aluminum (C-S-H) and with aluminum (C-A-S-H). Gel compounds are frequently found as metastable phases in this type of reaction, decreasing their stability with increasing temperature of reaction [36–38]. In some cases, they act as precursors to the formation of other stable phases such as stratlingite or zeolites [39].

The pH is the parameter that controls the Ca^{2+} (aq.) concentration in the solution. As the reaction evolved, the pH decreased, and the system reached a steady state in a time up to 28 days (age included as a limit in the cement standards applicable in this case).

In order to set the experimental conditions, a pilot experiment was initially designed that included natural kaolin calcined at 600 °C/2 h and treated with a saturated lime solution for one, seven, 28,

90, and 360 days. The pH and Ca^{2+} (aq.) concentrations (determined via EDTA titration and by ICP/MS spectrometry) were measured in the laboratory immediately after each extraction, at the end of the hydration reaction. Differences in both measures were linked to temperature dependence under high-pH conditions.

Figure 6 presents the Ca^{2+} (aq.) concentration evolution as a function of the experimental pH values obtained for each reaction time using both methods (EDTA titration and ICP/MS) and, in turn, variations in pH with regard to the Ca^{2+} concentrations measured for each reaction time experimentally and using the PHREEQC program.

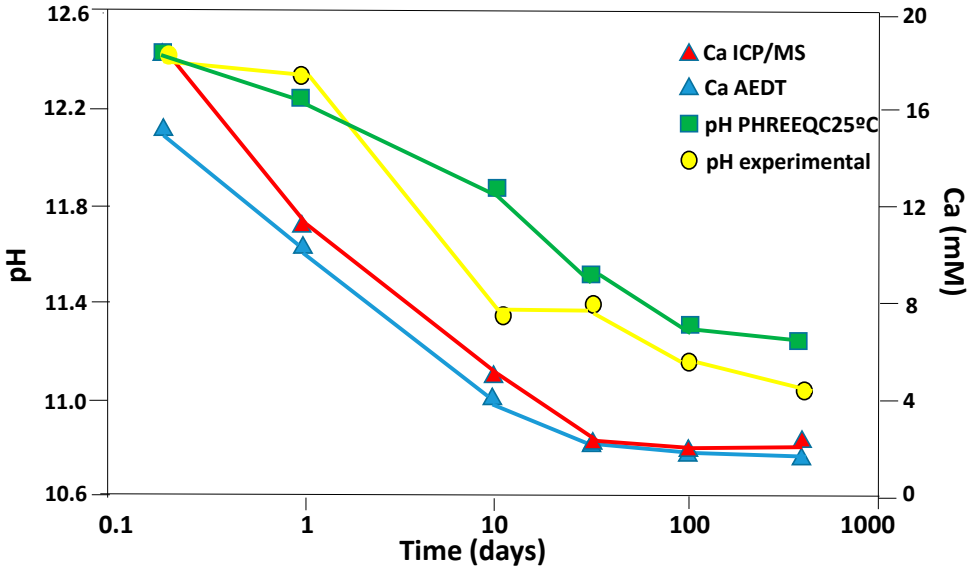

Figure 6. Behavior of Ca^{2+} (aq.) concentration and pH using different measurement methods.

No significant differences were observed regarding the Ca^{2+} concentration measured using both methods, except for the first set of data, carried out at six hours of reaction, which differed by more than three units (mM). Measurements of Ca^{2+} (aq.) depended on the temperature under conditions of high pH. In addition, it can be seen that the pozzolanic reaction ended after 28 days, since the Ca^{2+} concentration remained, from that moment, constant in the solution.

The pH calculated theoretically by the PHREEQC method progressively decreased up to 28 days of reaction in an order of magnitude from 12.4 to 11.4, and then remained in the range of 11.4/11.3. The observation was in accordance with the determinations made using Ca^{2+} (aq.) and confirmed that the ion availability controlled the reaction. However, the experimentally determined pH in the laboratory did not indicate the end of the hydration reaction nor did it justify values for long times (28, 90, and 360 days) whose pH differed from that calculated in the measurements performed after seven days (Figure 6).

ICP/MS analysis was the method used to measure the ion concentrations considered in this work at a constant ambient temperature, and the chemical speciation determined by this method was the one introduced in the PHREEQC program in order to optimize pH measurements at 25 °C.

The Ca^{2+} (aq.) concentration evolution with the reaction time for the thermally activated kaolin is shown in Figure 7. A Ca^{2+} concentration decrease in the solution was observed for 600 °C /2 h and 750 °C /2 h, with a rapid decrease up to 28 days and another, slower decrease on longer time scales. The pozzolanic reaction stabilized after 90 days, at which point the Ca^{2+} concentration remained almost constant in solution. In 750 °C /2 h conditions, Ca^{2+} content in the solution was lower for each reaction time.

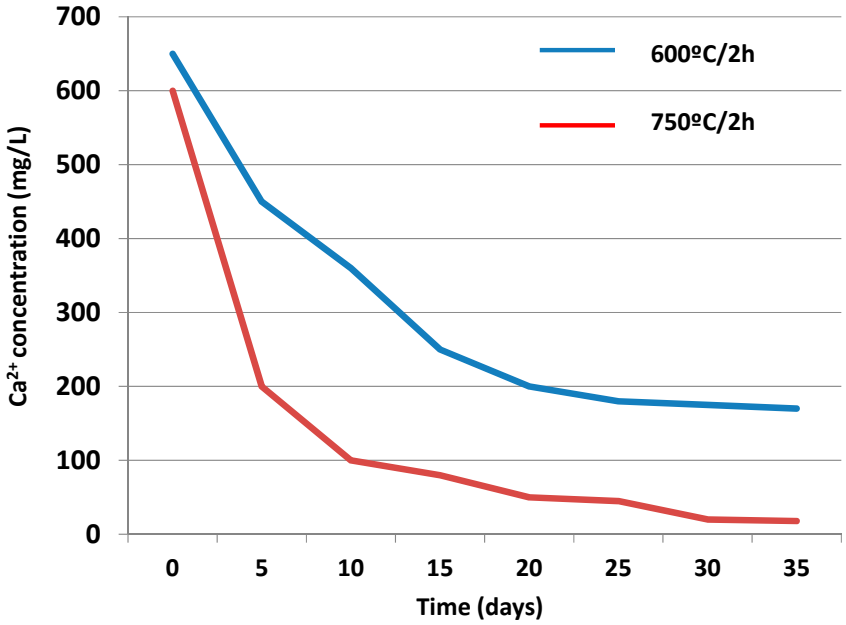

Figure 7. Behavior of Ca^{2+} concentration in the thermally activated kaolin systems.

At both temperatures, the rapid drop in Ca^{2+} concentration could be explained by the incorporation of the ions in these metastable structure phases, such as C-S-H gels and LDH-type compounds (phyllosilicate/carbonate), at short reaction times.

At longer time scales, i.e., 28, 90, and 360 days, metastable structures reorganized, evolving into stable phases. In these mechanisms, there was less calcium ion incorporation into the stable phases, which would explain the slower decrease in Ca^{2+} concentration in the solution. The activation at 750 °C/2 h enhanced the pozzolanic reaction, as reflected in the small Ca^{2+} content in the solution for all times.

When ZnO was added to the 600 °C/2 h and 750 °C/2 h systems, there was a slight decrease in Ca^{2+} (aq.) concentration in the solution, although the same trend was maintained regarding the evolution over time. The addition showed a similar behavior to Ca^{2+} (aq.) for Zn^{2+} (aq.), but with a lower content of Zn^{2+} in the solution (Figure 8).

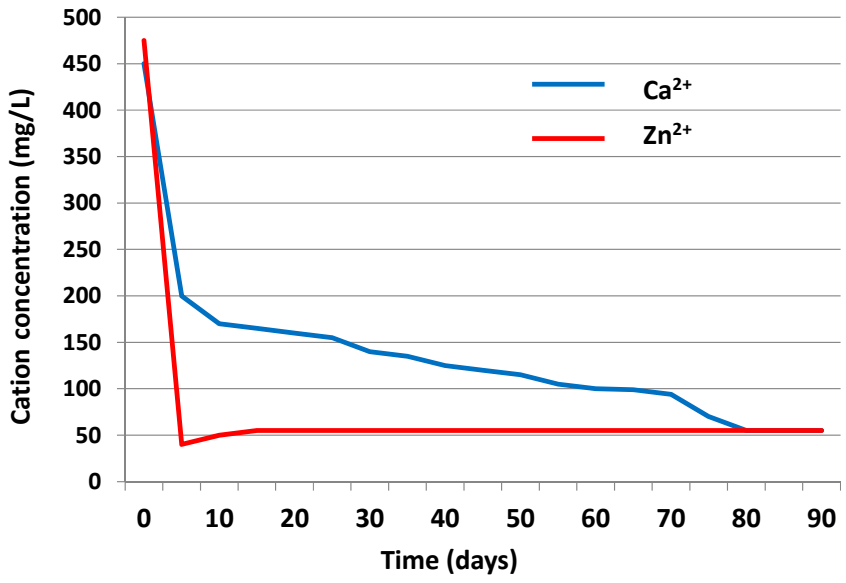

Figure 8. Behavior of Ca^{2+} and Zn^{2+} concentrations in the kaolin system activated at 600 °C/2 h.

These results agree with those obtained using SEM, where the presence of ZnO favored the incorporation of calcium and zinc in the pozzolanic reaction products. This behavior may explain the decrease in Ca^{2+} (aq.), compared to the samples without Zn^{2+}, where Zn^{2+} accompanying Ca^{2+} had a similar behavior, but with a lower content of ions in the solution [40]. The increment in temperature and reaction time increased these effects, since the reactivity of the activated phyllosilicates was major.

Aqueous silica and alumina provided additional information on the phase reaction with aluminosilicates. At both activation temperatures, the aqueous silica increased in solution up to 28 days and then decreased in all samples. However, the concentration range was still less than 0.1 mM, which is a very low value compared to the supposed content of reactive silica. These data suggest a rapid nucleation process of C-S-H gels on the reactive surface of MK, with little release of silica in the solution. The 750 °C/2 h conditions and the chemical activator presence did not seem to influence the behavior of aqueous silica (Figures 9 and 10).

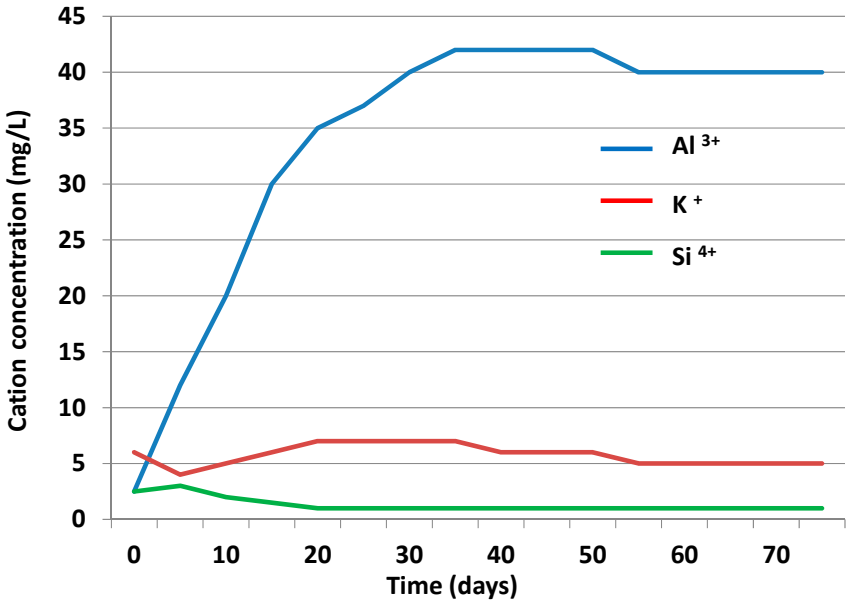

Figure 9. Behavior of ions during reaction in the kaolin activated at 600 °C/2 h.

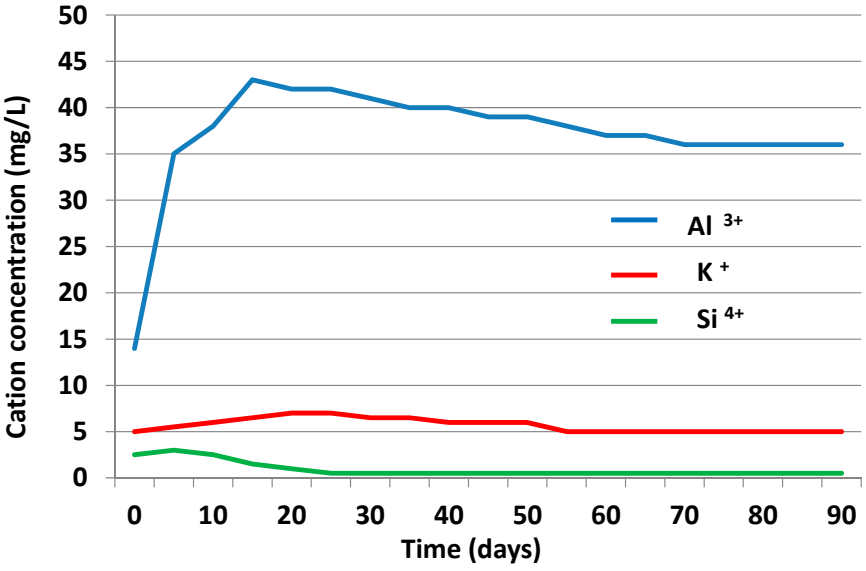

Figure 10. Behavior of ions during reaction in the kaolin activated at 750 °C/2 h.

At 600 °C /2 h and 750 °C /2 h, the aqueous alumina increased in solution during the first 28 days and remained almost constant in the 1.3/1.5 mM range on longer time scales. The presence of 1%

ZnO did not influence the behavior of the alumina in solution. The evolution of the aqueous alumina over time and the high concentration in solution suggest, in addition to a strong degradation of the primary minerals, the difficulty of the species of aqueous alumina (AlO_2^- in the alkaline medium) to be incorporated into the secondary minerals formed.

Aqueous K^+ concentration increased over time, suggesting its replacement by Ca^{2+} in the interlaminar region of the 2:1 phyllosilicates from natural kaolin and in the calcined materials. The K^+ concentration evolution in solution suggests that the process was favored by temperature and reaction time. The K^+ (aq.) content confirmed that it did not precipitate in any secondary form. Any soluble salt that may have been present in the initial solid sample was excluded, due to a correction made with the solutions through the reference solution. The presence of zinc helped the substitution of interlaminar potassium for calcium and zinc, which was incorporated into the 2:1 phyllosilicate structure. Aqueous Mg^{2+} and Na^+ did not show relevant information since their concentration was very small.

Calcite dissolution/precipitation reactions determine the carbonate and bicarbonate concentrations in solution and, therefore, the contribution of these species to alkalinity. It is assumed that the content of calcite present in the sample can have an influence on the chemistry of the solution, basically buffering the pH and, as a Ca^{2+} source, partially balancing the positive charge in the solution. Moreover, it should be considered that the exposure of the solution to the atmosphere, produced during the manipulation of the samples, leads to the partial carbonation of the solution [28].

3.4. Chemical Speciation of the Aqueous Phases: Use of the PHREEQC Code

The chemical speciation of the aqueous phases obtained after the saturated lime dissolution tests with natural and activated kaolin at seven, 28, 90, and 360 days, as well as the calculations of the system solubility, were performed using the reactive transport code PHREEQC [41].

The starting data employed to perform the speciation/solubility calculations were pH and total analytical concentrations obtained by ICP/MS at 25 °C of the dissolved species: Na^+, Mg^{2+}, AlO_2^-, K^+, Ca^{2+}, SiO_4^{2-}, and CO_3^{2-} of the pozzolanic assay (liquid phase). Mg^{2+} measurements made using ICP/MS showed amounts below the μM scale. In order to normalize its concentration, a 1×10^{-3} μM concentration was established at all times.

To obtain a prediction of the reaction product stability as a function of time, the saturation indices of the phases capable of being in a dissolved or precipitated state in the system were calculated with the code PHREEQC and the thermodynamic database, included in LLNL (Lawrence Livermore National Laboratories). Hydrated crystalline phases not included in LLNL were added from the THERMODDEM database to obtain a good compositional fit [42]. The selected minerals compositions studied were LDH-type compounds (phyllosilicate/carbonate) Si_2Al_2 (CO_3) $(OH)_{12}$, stratlingite Ca_2Al_2 (SiO_2) $(OH)_{10}$, muscovite $KAl_3Si_4O_{10}$ $(OH)_4$, Ca/Si gels = 0.8: $Ca_{0.8}SiO_{2.8}$, Ca/Si gels = 1.2: $Ca_{1.2}SiO_{3.2}$, and Ca/Si gels = 1.6: $Ca_{1.6}SiO_{3.6}$

Figures 11 and 12 compare the evolution of the saturation indices of the newly formed phases from the pozzolanic reaction for natural and activated kaolin.

Stratlingite, LDH-type compounds (phyllosilicate/carbonate), and muscovite with positive saturation indices were the phases with a trend to precipitate, coinciding with the experimental observations. C-S-H gels with higher Ca/Si ratios were thermodynamically predicted to be more stable in the short term (one day), being more unstable in the long term, which was justified by the Ca^{2+} (aq.) concentration.

When the Ca^{2+} (aq.) concentration was high, C-S-H gels = 1.8 were favored in their formation. As the reaction continued, the Ca^{2+} availability in the aqueous system was reduced and the C-S-H gel formations with lower Ca/Si ratios were those that existed thermodynamically. However, if kinetic considerations were taken into account, C-S-H gels with lower Ca/Si ratios would form faster, even allowing the incorporation of Ca^{2+} into an already formed C-S-H gel.

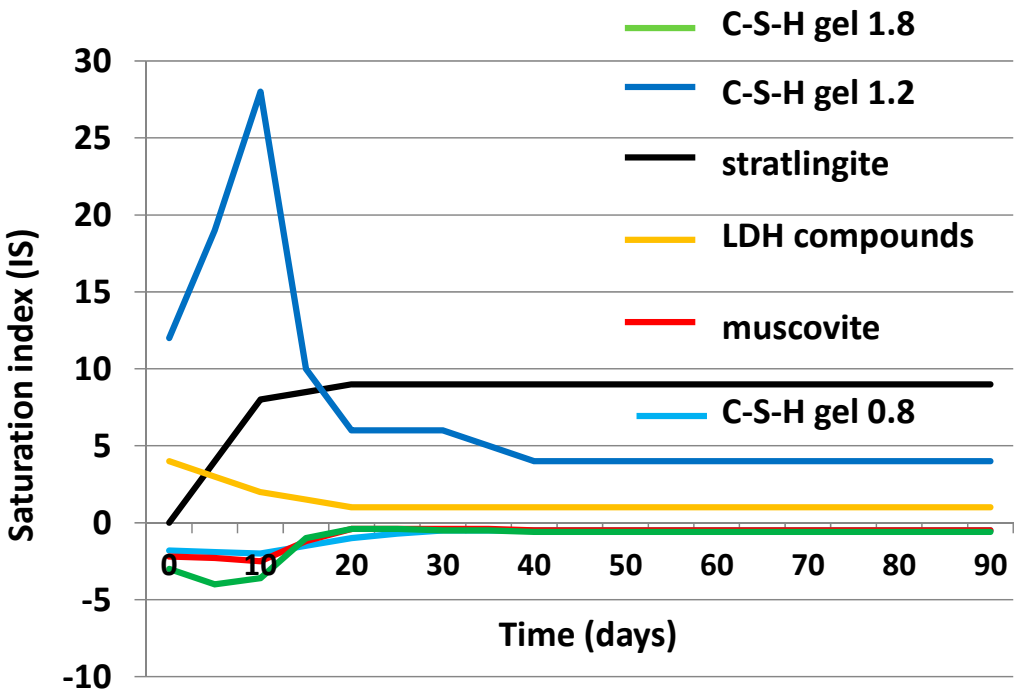

Figure 11. Saturation index from thermally activated kaolin.

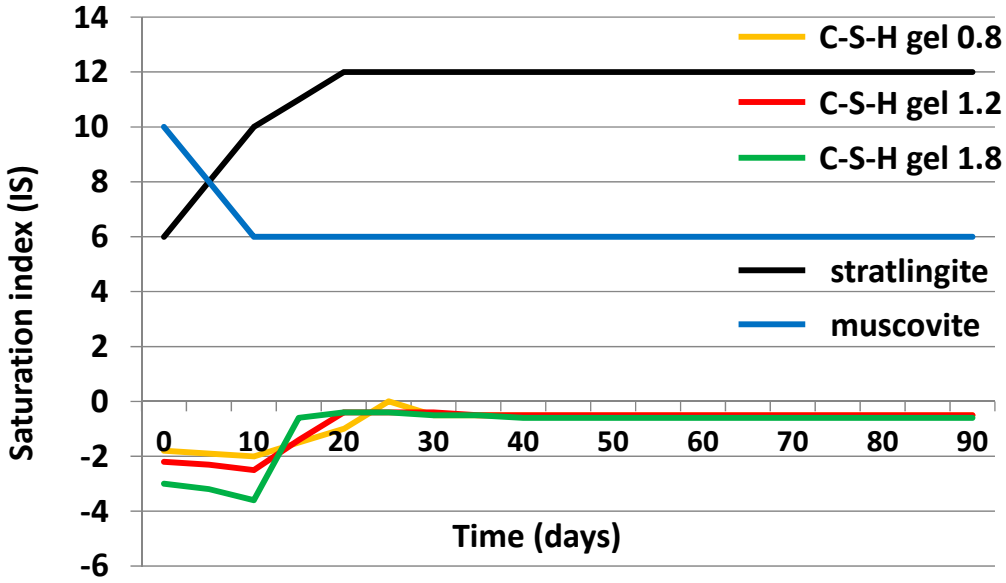

Figure 12. Saturation index from chemically and thermally activated samples.

On the other hand, the chemical and thermally activated sample simulations (Figure 12) had a similar behavior for stratlingite, muscovite-Ca, and C-S-H gels to that observed in natural kaolin. However, the presence of ZnO contributed to the LDH-type compound (phyllosilicate/carbonate) stability, with negative saturation indices not present in this moment.

From the temporal evolution of the IS obtained after the chemical speciation of the experimental aqueous phases, the most stable association in the system was defined, considering the neoformed phases in the pozzolanic reaction. As a criterion, it was established that the most stable phases had positive IS, that is, they were supersaturated in the aqueous phases analyzed, including compounds such as LDH (phyllosilicate/carbonate), stratlingite, and muscovite-Ca. C-S-H gels, int the amorphous phase close to equilibrium, were considered more stable. Despite the negative sign, it was established

that C-S-H gels with Ca/Si = 0.83 of the tobermorite type and composition $Ca_{0.83}$ SiO_2 $(OH)_{1.66}$ had a higher probability of formation.

The stability fields of the LDH-type compounds (phyllosilicate/carbonate) + stratlingite + C-S-H gels were evaluated for the products of the pozzolanic reactions of thermally activated kaolin. The stability fields of the muscovite + stratlingite + C-S-H gels were evaluated for the products of pozzolanic reactions from chemically and thermally activated kaolin since, under these conditions, the formation of LDH-type compounds (phyllosilicate/carbonate was inhibited.

The chemical stabilities of the experimental solutions were evaluated based on their stability fields with the SUPCRT92 simulation program [43]. The standard thermodynamic properties necessary to calculate the equilibrium constants of each reaction (ΔG° J/mol, ΔH° J/mol, S° J/mol·K, and V° cm^3/mol) and the Maier–Kelly coefficients (a, J/mol·K, b, J/mol·K^2, and c, J·K/mol) were determined [44].

Figure 13 shows the stability fields for the thermally activated kaolin with LDH compounds + stratlingite + C-S-H gel. The solutions at one day of reaction were located in the C-H-S gel stability field, while, at others times, these same solutions evolved toward the stratlingite field.

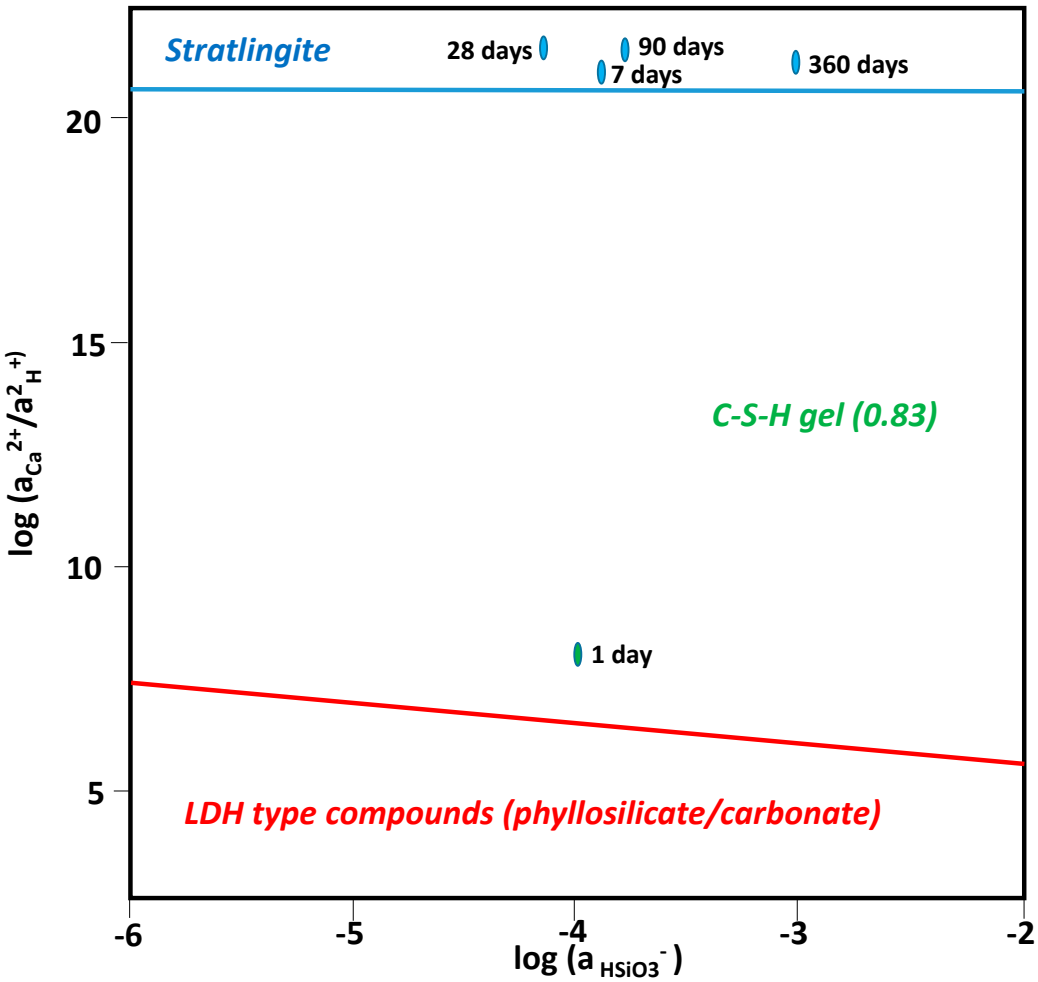

Figure 13. Plot of stability fields for LDH compounds + stratlingite + C-S-H gel system from the activated thermally kaolin systems.

In double activation chemical and thermal systems, the stability fields in the equilibrium were situated between C-S-H gels and stratlingite, between muscovite-Ca and C-S-H gels, and between stratlingite and muscovite-Ca (Figure 14).

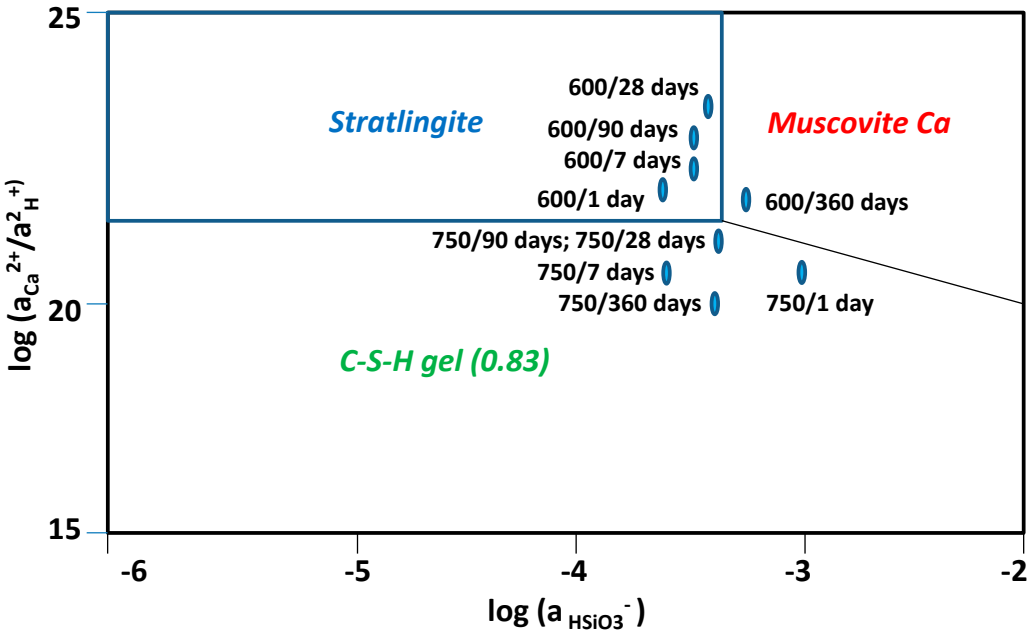

Figure 14. Plot of stability fields for muscovite Ca + stratlingite + C-S-H gel system from the chemically and thermally activated kaolin.

The solutions at one day of reaction were located inside the stability field of the muscovite-Ca, while, for the reaction times of seven, 28, 90, and 360 days, the solutions were inside the stratlingite field. At 750 °C/2 h, all the solutions representative of the reaction times were grouped in the stability field of C-S-H gels.

4. Conclusions

Natural kaolin is made up of kaolinite and muscovite aggregates with variable sizes. The surfaces are compact, showing the typical laminar appearance of these phyllosilicates. Superficial chemical analysis indicated a composition of silicon and aluminum in the kaolinite that conformed to the ideal structural formula of the 1:1 dioctahedral phyllosilicate. From mica, in addition to silicon and aluminum, iron, potassium, titanium, and magnesium also appeared, adjusting the structural formula to the 2:1 dioctahedral phyllosilicate, in which isomorphic substitutions of the tetrahedral and octahedral cations occurred.

Ca^{2+} in solution was incorporated into the structures of the metastable phases quickly up to 28 days of reaction, and then slowly into the stable phases, via replacement of K^{+} by Ca^{2+} in the interlaminar region of the 2:1 phyllosilicates, achieving the stability of the pozzolanic reaction from 90 days onward. The increases in temperature and chemical activator helped the interlaminar potassium's substitution into the 2:1 phyllosilicates and the Ca^{2+} and Zn^{2+} incorporation into their structures.

Low aqueous silica contents suggested a rapid nucleation phase of metastable phases with little release of silica to solution. The high concentration of aqueous alumina and its evolution in solution showed the mineral degradation that appeared in natural kaolin and the difficulty of aqueous alumina to incorporate into mineral phases. An increase in temperature and the presence of a chemical activator did not influence the behavior of these ions in solution.

Stability analysis from the kaolin/lime activated system showed that the C-S-H gels were thermodynamically stable after one day of reaction, evolving the system to the stratlingite stability field for the other analyzed times. In the chemically and thermally activated system at 600 °C/2 h, muscovite-Ca was the stable phase after one day of reaction, evolving toward stratlingite for the other analyzed times. At 750 °C/2 h, the C-S-H gels were the thermodynamically stable phases in the reaction.

The obtained material after chemical and thermal activation of natural kaolinite has a high pozzolanic activity and is suitable for use as a supplementary cementitious material in the manufacture of commercial cement. Calcination at 600 °C/2 h with 1% ZnO addition constitute the optimal conditions, improving the pozzolanic reaction and favoring the formation of stable reaction products, which directly influence the mechanical and durability properties of the material.

Author Contributions: Conceptualization, R.V.d.l.V.; methodology, I.S. and M.C.; software, I.S.d.S.; writing—original draft preparation, R.G.-G. All authors read and agreed to the published version of the manuscript.

Funding: This research received no external funding.

Conflicts of Interest: The authors declare no conflicts of interest.

References

1. Frias, M.; Vigil, R.; Garcia, R.; de Soto, I.; Medina, C.; Sánchez de Rojas, M.I. Scientific and technical aspects of blended cement matrices containing activated slate wastes. *Cem. Concr. Comp.* **2014**, *48*, 19–25. [CrossRef]
2. Juenger, M.C.G.; Siddique, R. Recent advances in understanding the role of supplementary cementitious materials in concrete. *Cem. Concr. Res.* **2015**, *78*, 71–80. [CrossRef]
3. Stark, A. Recent advances in the field of cement hydration and microstructure analysis. *Cem. Concr. Res.* **2011**, *41*, 666–678. [CrossRef]
4. Frias, M.; Sánchez de Rojas, M.I.; Rodríguez, O. Paper sludge, an environmentally sound alternative source of MK-based cementitious materials: A review. *Constr. Build. Mat.* **2015**, *74*, 37–48. [CrossRef]
5. Hewlett, P.C. *Lea´s Chemistry of Cement and Concrete*, 4th ed.; Elsevier Ltd.: Oxford, UK, 1992.
6. Rashad, S.A.M. Metakaolin as cementitious material: History, scours, production and composition—A comprehensive overview. *Constr. Build. Mat.* **2013**, *41*, 303–318. [CrossRef]
7. Van Damme, H. Concrete material science: Past, present, and future innovations. *Cem. Concr. Res.* **2018**, *112*, 5–24. [CrossRef]
8. Roussel, N. Rheological requirements for printable concretes. *Cem. Concr. Res.* **2018**, *112*, 76–85. [CrossRef]
9. Pera, J.; Ambroise, J.; Chabannet, M.; Chabannet, M. Transformation of wastes into complementary cementing materials. In Proceedings of the Seventh CANMET/ACI/JCI International Conference on Fly Ash, Silica Fume, Slag and Natural Pozzolans in Concrete, Madras, India, 1 January 2001; pp. 459–475.
10. Vegas, I.; Ureta, J.; Frias, M.; Rodríguez, O.; Garcia, R.; Vigil, R. *Scientific and Technical Aspects on the Use of Thermally Treated Paper Sludges in Cement*; Wascon: Lyon, France, 2006; pp. 519–530.
11. Rodríguez, O. Valorización de un Residuo Industrial Procedente de la Industria Papelera Como Material Puzolánico. Ph.D. Thesis, UAM, Madrid, Spain, 2008; p. 217.
12. Ferreiro, S. Activación Térmica del Lodo de Papel Estucado Para su Valorización Como Adición Puzolánica en la Industria Cementera. Ph.D. Thesis, Universidad de Castilla La Mancha, Ciudad Real, Spain, 2010; p. 262.
13. Sánchez de Rojas, M.I.; Marin, F.; Rivera, J.; Frias, M. Morphology and properties in blended cement with ceramic wastes as a pozzolanic material. *J. Am. Ceram. Soc.* **2006**, *89*, 3701–3705. [CrossRef]
14. Frias, M. Study of hydrated phases present in a MK-lime cured at 60 °C and 60 months of reaction. *Cem. Concr. Res.* **2006**, *36*, 827–831. [CrossRef]
15. Villar-Cociña, E.; Frias, M.; Valencia Morales, E.; Sánchez de Rojas, M.I. An evaluation of different kinetic models for determining the kinetic coefficients in sugar cane Straw-clay ash/lime system. *Adv. Cem. Res.* **2006**, *18*, 26–27. [CrossRef]
16. Organismo de Normalización España. *Métodos de Ensayo de Cementos. Parte V: Ensayo de Puzolanicidad para los Cementos Puzolánicos*; AENOR: Madrid, Spain, 2006.
17. Moore, M.; Reynolds, R.C. *X-ray Diffraction and the Identification and Analysis of Clay Minerals*, 2nd ed.; Oxford University Press: Oxford, UK, 1997.
18. Pera, J.; Amrouz, A. Development of highly reactive metakaolin from paper sludge. *Adv. Cem. Based Mat.* **1998**, *7*, 49–56. [CrossRef]
19. Vigil, R.; Frias, M.; Sánchez de Rojas, M.I.; Vegas, I.; Garcia, R. Mineralogical and morphological changes of calcined paper sludge at different temperatures and retention in furnace. *Appl. Clay Sci.* **2007**, *36*, 279–286. [CrossRef]

20. Vigil de la Villa, R.; Rodriguez, O.; Garcia, R.; Frias, M. Mineral phases in an activated kaolinitic waste blended cement system. *Appl. Clay Sci.* **2010**, *50*, 137–142. [CrossRef]
21. Garcia, R.; de la Villa, R.V.; Rodríguez, O.; Frias, M. Study of hydrated phases present in calcined paper sludge (metakaolinite)/saturated CaO dissolution system cured at 40 °C and 28 days of reaction. *Mat. Sci. Eng. A* **2010**, *527*, 3936–3941. [CrossRef]
22. Vigil de la Villa, R.; Frias, M.; Garcia Giménez, R.; Martinez Ramirez, S.; Fernández-Carrasco, L. Chemical and mineral transformations that occur in mine waste and washery rejects during pre-utilization calcination. *Int. J. Coal Geol.* **2014**, *132*, 123–130. [CrossRef]
23. García, R.; Vigil de la Villa, R.; Frías, M.; Rodríguez, O.; Martínez-Ramírez, S.; Fernández-Carrasco, L.; de Soto, I.S.; Villar Cociña, E. Mineralogical study of calcined coal waste in a pozzolan/Ca $(OH)_2$ system. *Appl. Clay Sci.* **2015**, *108*, 45–54. [CrossRef]
24. Ambroise, J.; Murat, M.; Pera, J. Investigations on synthetic binders obtained by middle-temperature thermal dissociation of clay minerals. *Silic. Indust.* **1986**, *7*, 99–107.
25. Sayanam, R.A.; Kalsotra, A.K.; Mehta, S.K.; Sing, R.S.; Mandal, G. Studies on thermal transformations and pozzolanic activities of clay from Jammu region (India). *J. Thermal Anal.* **1989**, *35*, 9–106. [CrossRef]
26. O´Farrell, M.; Sabir, B.B.; Wild, S. Strength and chemical resistance of mortars containing brick manufacturing clays subjected to different treatments. *Cem. Concr. Comp.* **2006**, *28*, 790–799. [CrossRef]
27. Frías, M.; Vigil de la Villa, R.; García, R.; Sánchez de Rojas, M.I.; Juan Valdés, A. The influence of slate waste activation conditions on mineralogical changes and pozzolanic behavior. *J. Am. Ceram. Soc.* **2013**, *96*, 1–7. [CrossRef]
28. Brindley, G.W.; Brown, G. *Crystal Structures of Clay Minerals and their X-ray Identification*; Mineralogical Society Monograph: London, UK, 1980.
29. Santos Silva, A.; Gameiro, A.; Grillo, J.; Veiga, R.; Velosa, A. Long-term behaviour of lime-metakaolin pastes at ambient temperature and humic curing condition. *Appl. Clay Sci.* **2014**, *88–89*, 49–55. [CrossRef]
30. Shi, C.; Grattan-Bellew, P.E.; Stegemann, J.A. Conversion of a waste mud into a pozzolanic material. *Constr. Build. Mat.* **1999**, *13*, 279–284. [CrossRef]
31. Favier, A.; Habert, G.; D'Espinose de Lacaillerie, J.B.; Roussel, N. Mechanical properties and compositional heterogeneities of fresh geopolymer pastes. *Cem. Concr. Res.* **2013**, *48*, 9–16. [CrossRef]
32. Favier, A.; Habert, G.; Roussel, N.; D'Espinose de Lacaillerie, J.B. A multinuclear static NMR study of geopolymerisation. *Cem. Concr. Res.* **2015**, *75*, 104–109. [CrossRef]
33. Abdolhosseini Qomi, M.; Krakowiak, K.; Bauchy, M.; Stewars, K.L.; Shahsavari, R.; Jagannathan, D.; Brommer, D.B.; Baronnet, A.; Buehler, M.J.; Yip, S.; et al. Combinatorial molecular optimization of cement hydrates. Combinatorial molecular optimization of cement hydrates. *Nat. Commun.* **2014**, *5*, 4960. [CrossRef] [PubMed]
34. García, R.; Vigil de la Villa, R.; Vegas, I.; Frías, M.; Sánchez de Rojas, M.I. The pozzolanic properties of paper sludge waste. *Constr. Build. Mat.* **2008**, *22*, 1484–1490. [CrossRef]
35. Frias, M.; Rodríguez, O.; Nebreda, B.; Garcia, R.; Villar-Cociña, E. Influence of activation temperature of kaolinite-based clay wastes on the pozzolanic activity and kinetic parameters. *Adv. Cem. Res.* **2010**, *22*, 135–142. [CrossRef]
36. Ioannidou, K.; Pellenq, R.J.M.; del Gado, E. Controlling local packing and growth in calcium–silicate–hydrate gels. *Soft Matter* **2014**, *8*, 1121–1130. [CrossRef]
37. Ioannidou, K.; Krakowiak, K.J.; Bauchy, M.; Hoover, C.G.; Masoero, E.; Yip, S.; Ulm, F.J.; Levitz, P.; Pellenq, R.J.M.; del Gado, E. Mesoscale texture of cement hydrates. *Proc. Natl. Acad. Sci. USA* **2016**, *113*, 2029–2034. [CrossRef]
38. Ioannidou, K.; Kanduc, M.; Li, L.; Frenkel, D.; Dobnikar, J.; Flenkel, D.; Del Gado, E. The crucial effect of early-stage gelation on the mechanical properties of cement hydrates. *Nat. Commun.* **2016**, *7*, 12106. [CrossRef]
39. De Silva, P.S.; Glasser, F.P. Phase relations in the system CaO-Al_2O_3-SiO_2-H_2O relevant to MK-Calcium Hydroxide. *Cem. Concr. Res.* **1993**, *23*, 627–639. [CrossRef]
40. Nicoleau, L.; Nonat, A. A new view on the kinetics of tricalcium silicate hydration. *Cem. Concr. Res.* **2016**, *86*, 1–11. [CrossRef]

41. Parkhurst, D.L.; Appelo, C.A.J. User´s guide to PHREEQC (version 2). In *A Computer Program for Speciation, Batch-Reaction, One-Dimensional Transport, and Inverse Geochemical Calculations*; US Geological Survey: Reston, VA, USA, 1999; p. 312.
42. Blanc, P.; Lassin, A.; Piantone, P.; Burnol, A. *Thermoddem a Database Devoted to Waste Minerals*; BRGM: Orleans, France, 2007; p. 6009. Available online: http://thermoddem.brgm.fr (accessed on 10 June 2020).
43. Johnson, J.W.; Oelkers, E.H.; Helgeson, H.C. SUPCRT92: A software package for calculating the standard molal thermodynamic properties of minerals, gases, aqueous species, and reactions from 1 to 5000 bar and 0 to 1000 °C. *Comput. Geosci.* **1992**, *18*, 899–947. [CrossRef]
44. Lothenbach, B.; Matschei, T.; Möschner, G.; Glasser, F.P. Thermodynamic modelling of the effect of temperature on the hydration and porosity of Portland cement. *Cem. Concr. Res.* **2008**, *38*, 1–18. [CrossRef]